

Supplementary Materials

Surface N-type Band Bending for Stable Inverted CsPbI₃ Perovskite Solar Cells with over 20% Efficiency

Shuo Wang, ^{†,a} *Ming-Hua Li*, ^{†,a} *Yanyan Zhang*, ^a *Yan Jiang*, ^{b,*} *Li Xu*, ^c *Fuyi Wang*, ^{a, d}
and *Jin-Song Hu*, ^{a,d,*}

^a Dr. S. Wang, Dr. M.-H. Li, Y.-Y. Zhang, Prof. F.-Y Wang, Prof. J.-S. Hu

Beijing National Laboratory for Molecular Sciences (BNLMS), Institute of Chemistry,
Chinese Academy of Sciences, Beijing 100190, China

^b Prof. Y. Jiang

School of Materials Science and Engineering, Beijing Institute of Technology, Beijing
100081, China

^c Dr. L. Xu

Beijing Institute of Smart Energy, Beijing 102299, China

^d Prof. F.-Y Wang, Prof. J.-S. Hu

University of Chinese Academy of Sciences, Beijing 100049, China

* Corresponding author: yan.jiang@bit.edu.cn (Y. J.), hujs@iccas.ac.cn (J. H.)

[†] S. W. and M.-H. L. contributed equally to this work.

Materials

Poly [3-(4-carboxybutyl)thiophene-2,5-diyl] (P3CT, Mw: 30-40k) was obtained from Rieke Metals. HPbI₃ was purchased from Xi'an Polymer Light Technology Corp. [6,6]-Phenyl-C61-butyric acid methyl ester (PCBM) was purchased from Advanced Election Technology Co., Ltd. Cesium iodide (CsI, 99.999%), bathocuproine (BCP), dimethyl sulfoxide (DMSO, anhydrous, ≥99.9%), N, N-Dimethylformamide (DMF), chlorobenzene (anhydrous, 99.8%) and isopropyl alcohol (IPA) were purchased from Sigma-Aldrich and used as received. Propylamine hydrochloride (PACl, >98.0%),

Methylamine hydrochloride (MACl, >98.0%), Isopropylamine Hydrochloride (iPACl, >98.0%) and Butylamine Hydrochloride (BACl, >98.0%) were obtained from TCI. All the raw materials were used without any post process.

Devices Fabrication

The FTO glasses ($2 \times 2 \text{ cm}^2$) were ultrasonically cleaned and treated with UV-ozone for 20 minutes before use. The P3CT (0.5 mg/mL in DMF) HTLs were deposited by spin-coating at 4000 rpm for 20 s, the obtained P3CT films were annealed at 150°C for 10 min. The CsPbI₃ precursor solution (0.74 M, HPbI₃ and CsI in 1 mL DMF) were coated on FTO/P3CT substrates (preheated at 70 °C) by 2000 rpm for 30 s in N₂ glove box, followed by the annealing at 70°C for 3 min in N₂ condition and then 180°C for 20 min in air condition to obtain the CsPbI₃ films. Afterwards, the CsPbI₃ films were taken into the glove box for surface treating. PACl/IPA (1 mg/mL) was spin-coated onto the CsPbI₃ films at 3000 rpm for 20 s and annealed at 100°C for 2 min. The PCBM (20 mg/mL in CB) ETL was subsequently deposited on CsPbI₃ films at 3000 rpm for 30 s, followed by the deposition of BCP (0.5 mg/mL) at 3000 rpm for 30 s. Finally, a 100 nm Ag layer were thermally evaporated with a mask to complete the fabrication of the device with a defined active area of 0.09 cm².

Characterization

The optical absorption spectra were recorded by UV/vis spectrophotometer (Lambda 1050). The morphology of the perovskite film was captured by Field-Emission Scanning Electron Microscope (Hitachi, SU4800). The XRD diffraction patterns were collected on Rigaku DMAX-RB with a Cu-K α X-ray radiation source. Steady-state photoluminescence was conducted on a fluorescence spectrophotometer (HORIBA, FluoroMax+) and time-resolved photoluminescence spectra were recorded by Edinburgh Instruments (FLS980) with an excitation of 483 nm. The J-V curves were measured by ORIEL measurement system with a Keithley 2420 sourcemeter under simulated AM 1.5G irradiation (100 mW/cm²) in glove box, the devices were tested in N₂ condition. For stability tests, the devices were all aged in N₂ atmosphere. For

photostability tests, the devices were kept under continuous LED illumination (OPPLE) in N₂ condition. The impedance spectroscopy was performed by using an electrochemical workstation (CHI 660E) in dark condition at 1 V between the range from 1 MHz to 100 Hz. Mott-Schottky curves were tested at 10 kHz by using an electrochemical workstation (CHI 660E) in dark condition. The EQE spectra were tested by QE-R3011 (Enlitech) measurement system. The X-ray photoelectron spectroscopy (XPS) and ultraviolet photoelectron spectroscopy (UPS) were performed using an XPS/UPS system (Thermo Fisher Scientific, ESCALAB250XI). The TOF-SIMS analysis was performed with a TOF-SIMS 5 instrument (ION-ToF GmbH, Münster, Germany). A 30 keV Bi⁺ primary ion gun with a beam current of 0.95 pA was used for analysis and scanned on an area of 100×100 μm². A 10 keV Ar₁₇₀₀⁺ ion source with a beam current of 6.5 nA was used to sputter a crater of 300×300 μm². The dual-beam depth profiling was conducted in positive and negative ion modes, respectively. A low energy electron flood gun was adopted for charge compensation. Inverse photoemission spectroscopy (IPES) measurement was performed using a customized ULVAC-PHI LEIPS instrument with Bremsstrahlung isochromatic mode.

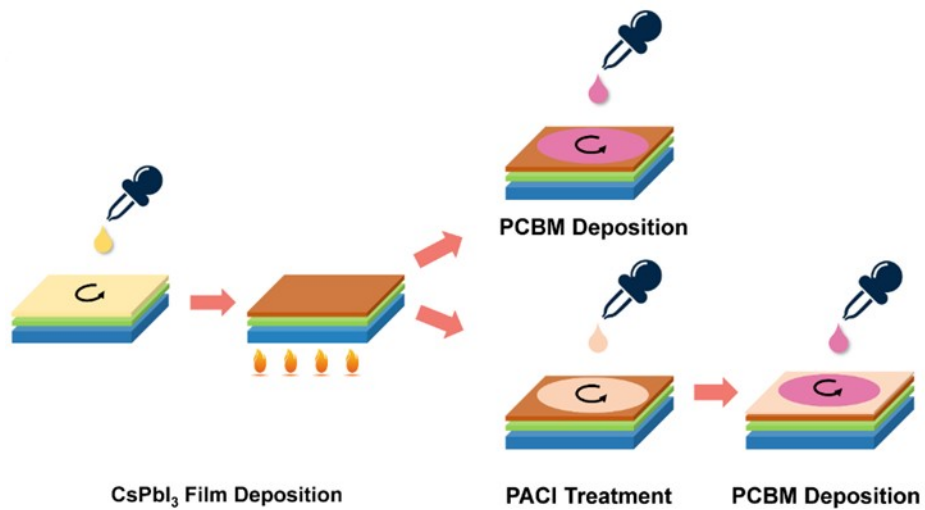


Fig. S1. Schematic of the deposition process of CsPbI₃ device.

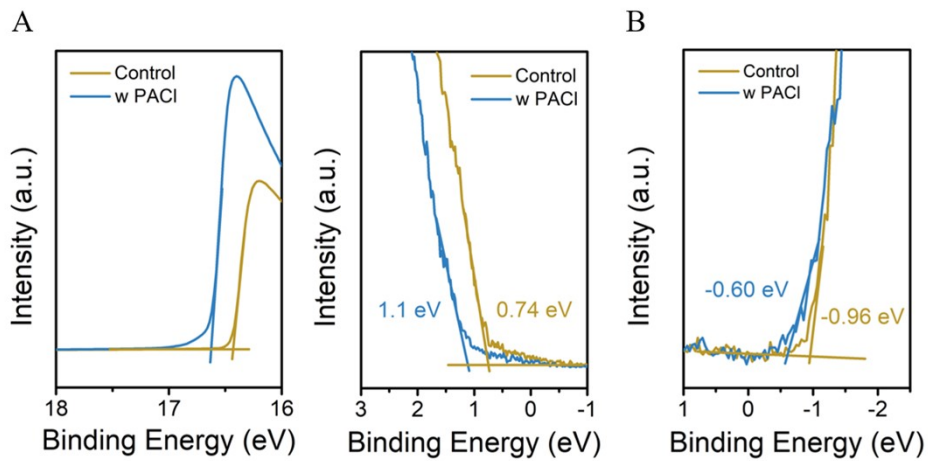


Fig. S2. (A) UPS and (B) IPES spectra of the CsPbI₃ films.

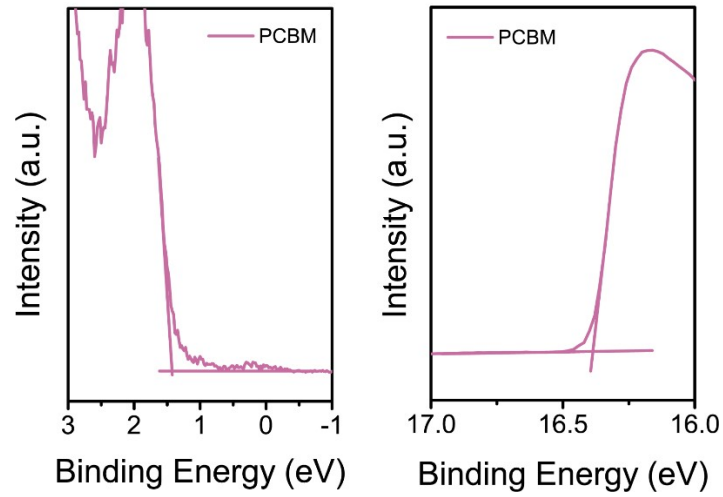


Fig. S3. UPS spectra of PCBM films.

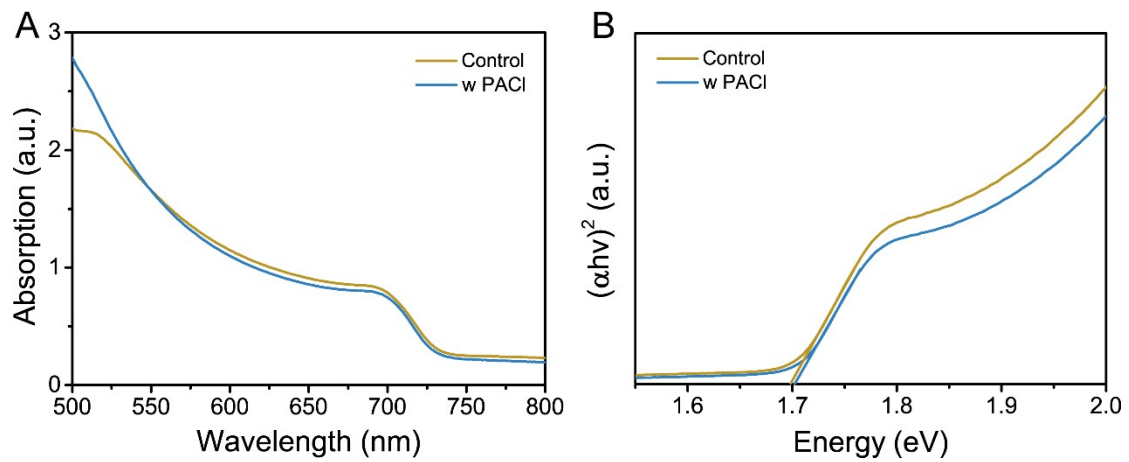


Fig. S4. (A) UV-vis spectra, (B) Tauc plots of the various CsPbI₃ films.

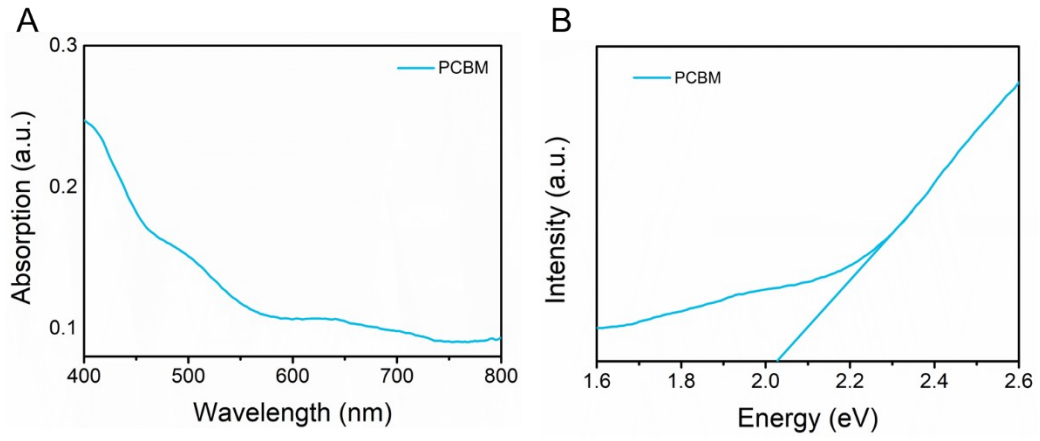


Fig. S5. (A) UV-vis spectrum and (B) Tauc plot of the PCBM film.

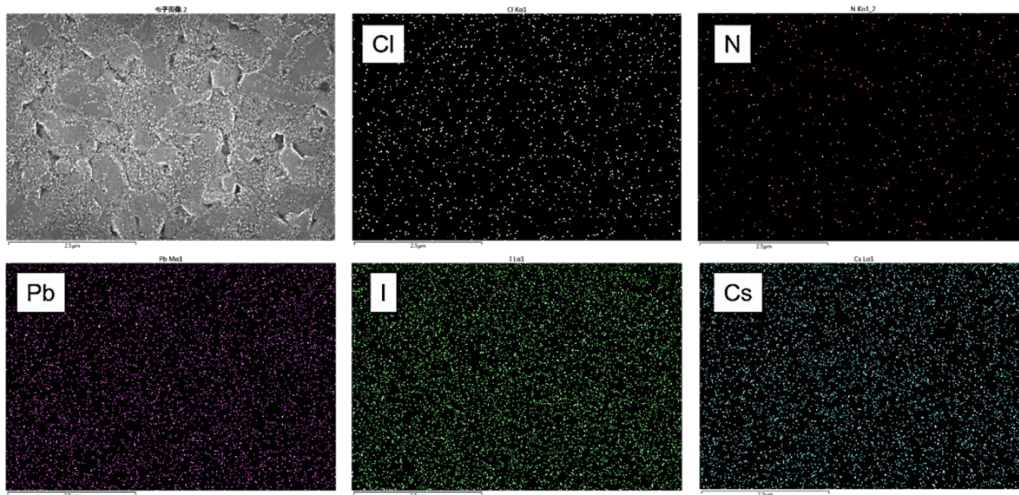


Fig. S6. EDX mapping of the w PACl film.

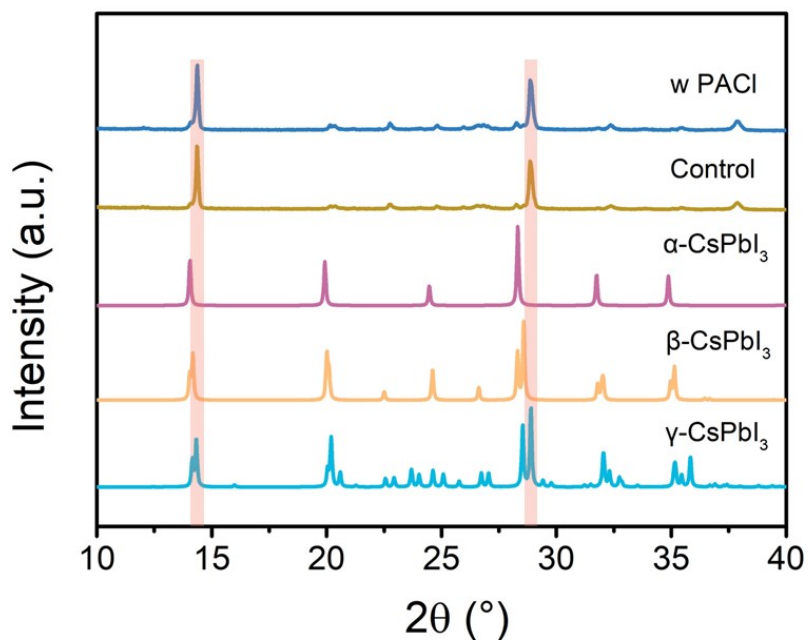


Fig. S7. Comparison of XRD patterns of the control and w PACI films with the standard XRD patterns of α , β , γ - CsPbI₃ obtained from the reference.¹

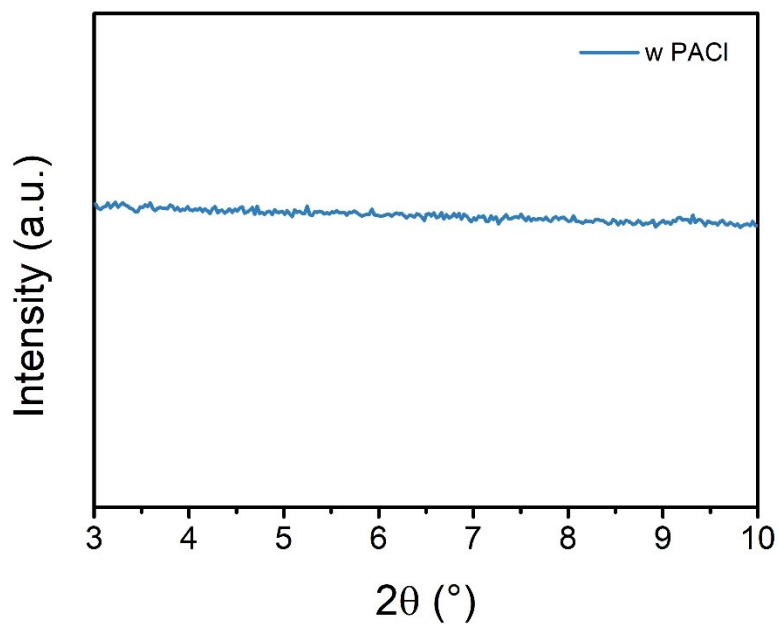


Fig. S8. XRD pattern of the w PACI sample from 3° to 10° .

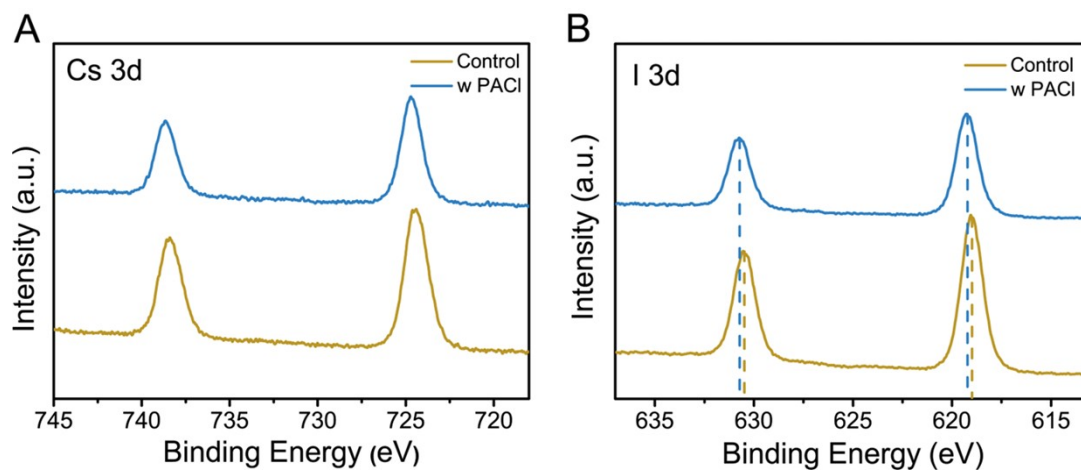


Fig. S9. XPS spectra of the control and w PACl films: (A) Cs 3d, (B) I 3d.

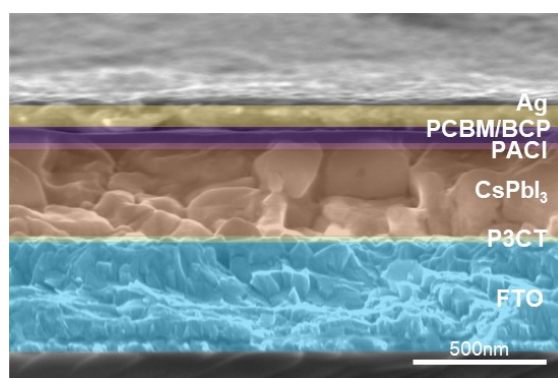


Fig. S10. Cross-section SEM image of the CsPbI₃ device with PACl.

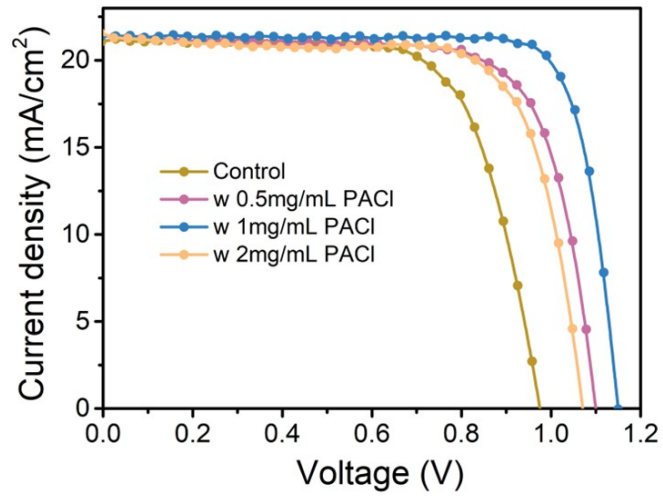


Fig. S11. J-V curves of the CsPbI₃ devices with different concentration of PACI.

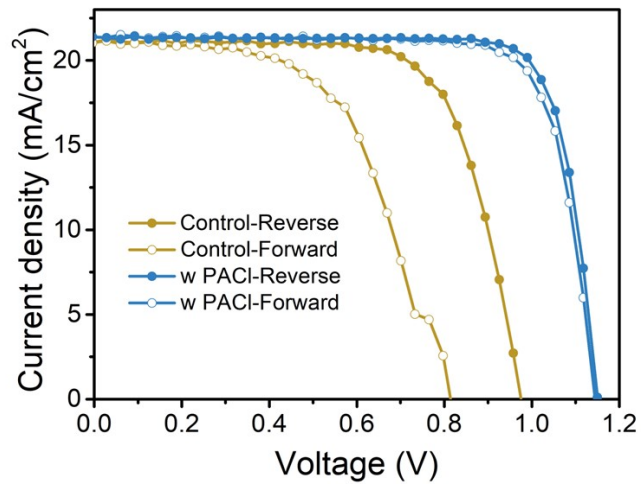


Fig. S12. J-V curves of the CsPbI₃ devices at different scan directions.

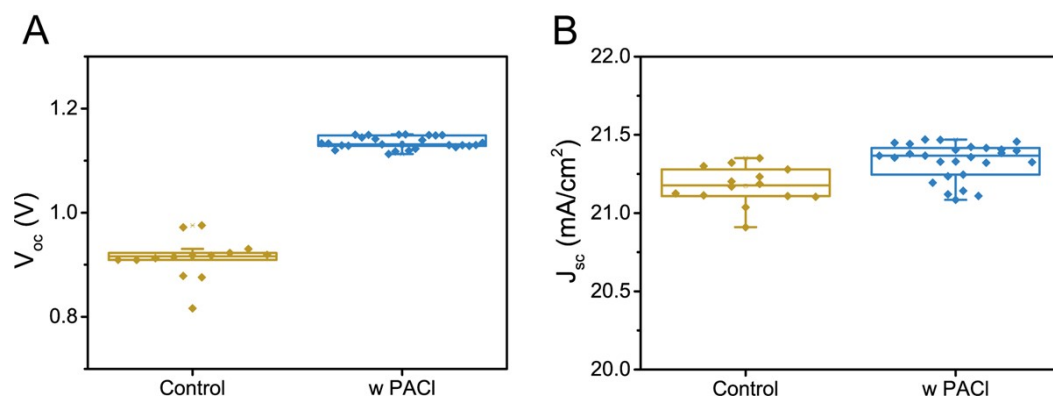


Fig. S13. Parameters distribution of the control devices and w PACI devices: (A) V_{oc} , (B) J_{sc} .

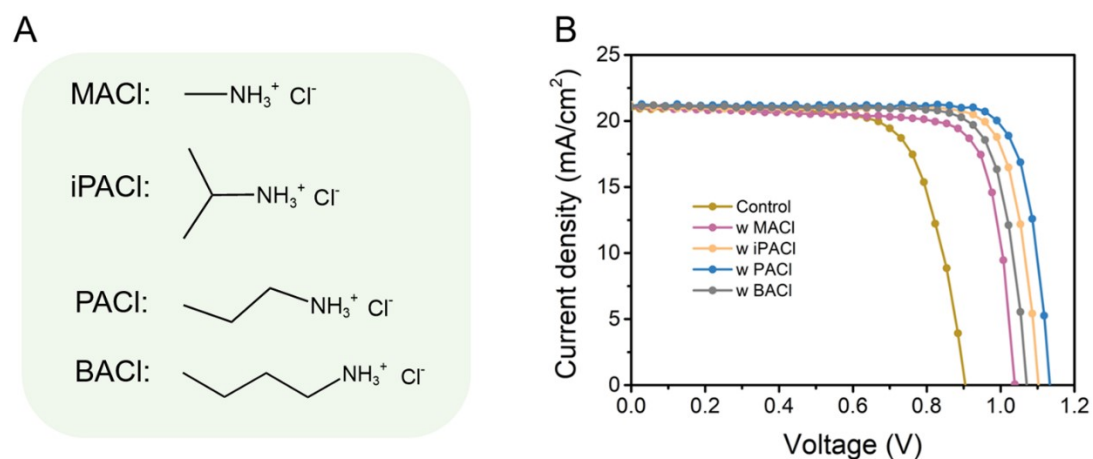


Fig. S14. The performance of the CsPbI₃ device treated with different Cl⁻ contained organic ammonium salts: (A) molecule structure of the Cl⁻ contained organic ammonium salts, (B) J-V curves of the CsPbI₃ devices.

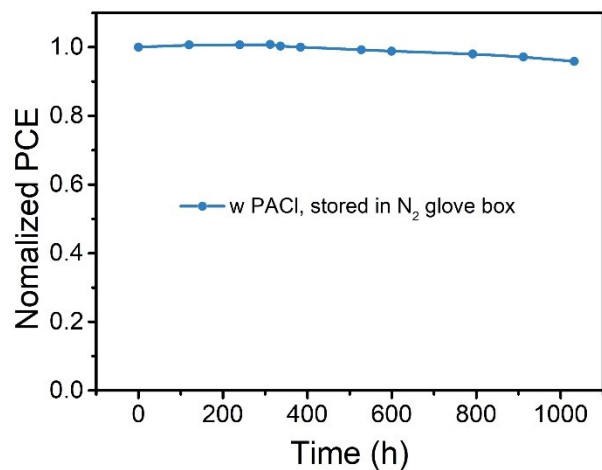


Fig. S15. Evolution of normalized PCE of the w PACI CsPbI₃ PSC. The device was stored in N₂ for 1032 h.

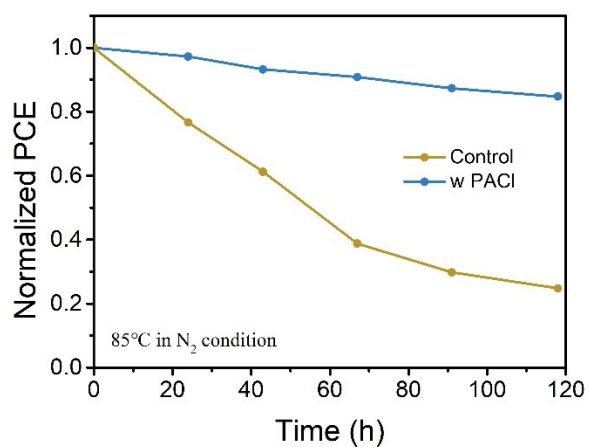


Fig. S16. Evolution of normalized PCE of the CsPbI₃ PSCs. The devices were stored in N₂ at 85 °C for about 120 h.

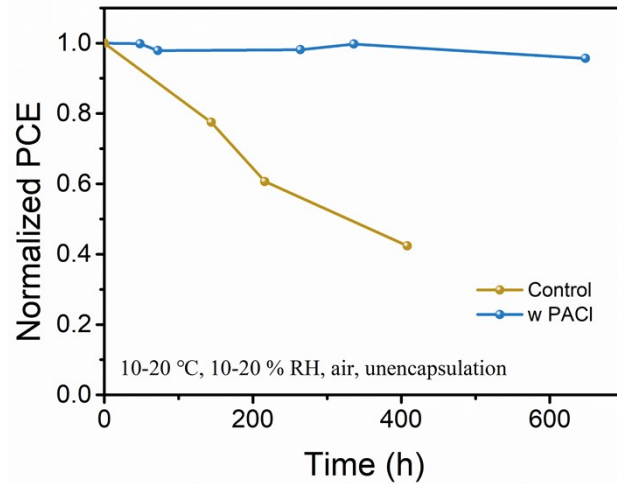


Figure S17. Evolution of normalized PCE of CsPbI₃ PSCs. The devices were stored under ambient atmosphere without encapsulation.

Table S1. The differences between our strategy and S. Fu et al.'s work.

	Energy level management	Defect passivation	Ref.
1	NA	Pb vacancy (V_{Pb}) traps I-Pb inversion (I_{Pb}) traps	<i>Adv. Mater.</i> 2022 , 34(38): 2205066
2	Surface n-type bending	Under-coordinated Pb^{2+} traps	This work

Table S2. Fitted results of time-resolved PL decay curves.

	τ_1 (ns)	τ_2 (ns)	A_1 (%)	A_2 (%)	$\tau_{average}$ (ns)
Control	1.30	22.18	0.35	0.65	14.87
w PACl	15.50	91.30	36.7	63.3	63.25

Table S3. Summary of photovoltaic performance of the CsPbI₃ device with different concentration of PACl.

	J_{sc} (mA/cm ²)	V_{oc} (V)	FF	PCE (%)
Control	21.12	0.97	0.70	14.43

w 0.5 mg/mL	21.35	1.10	0.73	17.23
w 1 mg/mL	21.39	1.15	0.82	20.11
w 2 mg/mL	21.35	1.07	0.73	16.68

Table S4. Summary of photovoltaic performance of the champion CsPbI₃ device.

	J _{sc} (mA/cm ²)	V _{oc} (V)	FF	PCE (%)
Control	21.12	0.97	0.70	14.43
w PACl	21.36	1.13	0.84	20.17

Table S5. Summary of photovoltaic parameters of inverted CsPbI₃ PSCs.

Device Structure	Year	V _{oc} (V)	FF	PCE (%)	Ref.
ITO/PTAA/CsPbI ₃ /PCBM/C ₆₀ /BCP/Cu or Al	2017	1.08	0.70	11.4	2
FTO/PTAA/CsPbI ₃ (OTG3)/PCBM/BCP/Ag	2019	1.12	0.75	13.32	3
ITO/P3CT- N/CsPbI ₃ /MAPyA/PCBM/C ₆₀ /BCP/Ag	2020	1.074	0.77	16.67	4
ITO/P3CT-N/CsPbI ₃ (w Si-Cl) /PCBM/C ₆₀ /BCP/Ag	2021	1.176	0.80	18.93	5
ITO/P3CT-N/CsPbI ₃ (w MAAD) /PCBM/C ₆₀ /BCP/Ag	2022	1.16	0.81	19.25	6
ITO/PTAA/CsPbI ₃ (OMXene)/CPTA/BCP/Ag	2022	1.21	0.82	19.69	7
ITO/P3CT-N/CsPbI ₃ (w FBJ)/PCBM/C ₆₀ /BCP/Ag	2022	1.225	0.77	19.27	8
ITO/P3CT- N/CsPbI ₃ /DAB/PCBM/C ₆₀ /BCP/Ag	2022	1.213	0.80	19.84	9
FTO/P3CT/CsPbI ₃ /PACl/PCBM/BCP/Ag	2022	1.13	0.84	20.17	this study

Table S6. Summary of photovoltaic performance of the CsPbI₃ device at different scan directions.

	J _{sc} (mA/cm ²)	V _{oc} (V)	FF	PCE (%)
--	---------------------------------------	---------------------	----	---------

Control	Reverse	21.12	0.97	0.70	14.43
	Forward	21.07	0.81	0.57	9.87
w PACl	Reverse	21.35	1.15	0.81	19.97
	Forward	21.43	1.14	0.79	19.31

Table S7. Summary of photovoltaic performance for CsPbI₃ PSCs with PACl.

	J _{sc} (mA/cm ²)	V _{oc} (V)	FF	PCE (%)
1	21.32	1.130	0.75	18.22
2	21.32	1.117	0.78	18.61
3	21.35	1.119	0.78	18.72
4	21.40	1.112	0.81	19.40
5	21.46	1.122	0.80	19.46
6	21.36	1.131	0.81	19.64
7	21.32	1.139	0.81	19.76
8	21.42	1.141	0.81	19.87
9	21.37	1.149	0.81	19.92
10	21.38	1.149	0.81	19.95
11	21.35	1.150	0.81	19.97
12	21.46	1.148	0.81	20.06
13	21.41	1.144	0.81	20.01
14	21.44	1.149	0.81	20.09
15	21.40	1.150	0.81	20.04
16	21.39	1.149	0.81	20.11
17	21.44	1.129	0.83	20.15
18	21.36	1.130	0.84	20.17
19	21.08	1.125	0.82	19.59
20	21.14	1.129	0.81	19.40
21	21.24	1.129	0.81	19.49
22	21.32	1.119	0.81	19.51
23	21.11	1.128	0.82	19.62
24	21.10	1.132	0.80	19.16
25	21.45	1.129	0.82	20.09

26	21.19	1.133	0.82	19.91
27	21.23	1.134	0.82	19.99

Table S8. Summary of photovoltaic performance of the CsPbI₃ device treated with different Cl⁻-contained organic ammonium salts.

	J _{sc} (mA/cm ²)	V _{oc} (V)	FF	PCE (%)
Control	20.93	0.905	0.72	13.69
w MACl	21.08	1.038	0.79	17.21
w iPACl	21.07	1.102	0.82	19.10
w PACl	21.19	1.133	0.83	19.92
w BACl	21.15	1.071	0.80	18.23

Table S9. Summary of indoor-photovoltaic performance of the CsPbI₃/PACl device measured under various light intensity.

Light source (lux)	P _{in} (μW/cm ²)	J _{sc} (μA/cm ²)	V _{oc} (V)	FF	P _{out} (μW/cm ²)	PCE (%)
250	76	32.9	0.97	0.81	25.7	33.82
500	153.5	70.1	0.99	0.82	57	37.13
1000	307	143	1.02	0.82	119.5	38.93

References

1. A. Marroñier, G. Roma, S. Boyer-Richard, L. Pedesseau, J.-M. Jancu, Y. Bonnassieux, C. Katan, C. C. Stoumpos, M. G. Kanatzidis and J. Even, *ACS Nano*, 2018, **12**, 3477-3486.
2. Q. Wang, X. Zheng, Y. Deng, J. Zhao, Z. Chen and J. Huang, *Joule*, 2017, **1**, 371-382.
3. T. Wu, Y. Wang, Z. Dai, D. Cui, T. Wang, X. Meng, E. Bi, X. Yang and L. Han, *Adv. Mater.*, 2019, **31**, 1900605.
4. S. Fu, L. Wan, W. Zhang, X. Li, W. Song and J. Fang, *ACS Energy Lett.*, 2020,

- 5**, 3314-3321.
5. S. Fu, W. Zhang, X. Li, J. Guan, W. Song and J. Fang, *ACS Energy Lett.*, 2021, **6**, 3661-3668.
 6. S. Fu, X. Li, J. Wan, W. Zhang, W. Song and J. Fang, *Adv. Funct. Mater.*, 2022, **32**, 2111116.
 7. J. H. Heo, F. Zhang, J. K. Park, H. J. Lee, D. S. Lee, S. J. Heo, J. M. Luther, J. J. Berry, K. Zhu and S. H. Im, *Joule*, 2022, **6**, 1672-1688.
 8. S. Fu, N. Sun, J. Le, W. Zhang, R. Miao, W. Zhang, Y. Kuang, W. Song and J. Fang, *ACS Appl. Mater. Interfaces*, 2022, **14**, 30937-30945.
 9. S. Fu, J. Le, X. Guo, N. Sun, W. Zhang, W. Song and J. Fang, *Adv. Mater.*, 2022, **34**, 2205066.